Phase Change in Azobenzene Derivative-Doped Liquid Crystal Controlled by the Photochromic Reaction of the Dye

Katarzyna Matczyszyn* and Juliusz Sworakowski

Institute of Physical and Theoretical Chemistry, Wroclaw University of Technology, Wyb. Wyspianskiego 27, PL-50-370 Wroclaw 51, Poland

Received: September 11, 2002; In Final Form: February 26, 2003

This contribution presents results of kinetic studies of the isomerization of photochromic 4-fluoro-4′-methoxyazobenzene dissolved in the liquid-crystalline pentylcyanobiphenyl (5CB). Deviations from the expected Arrhenius behavior were observed for the thermal cis−trans reaction near the phase transition temperature of 5CB. The activation energy of the thermal cis−trans isomerization (92 kJ/mol) and the preexponential factor (1.5×10^{11} s^{-1}) are lower than the respective values determined for the same dye dissolved in common solvents, apparently scaling with the polarity of the solvent. It was also found that the trans−cis isomerization results in the appearance of the isotropic phase at temperatures substantially lower than the thermodynamic nematic−isotropic phase transition temperature. A model, relating the kinetics of the isomerization to characteristic times of the phase transition has been put forward. The model takes into account differences in the solubility of both forms in the liquid-crystalline matrix, resulting from different compatibilities of their molecular shapes with that of 5CB.

Introduction

There has been a growing interest in properties of photoactive dye-doped liquid crystals owing to their emerging applications as information processing materials.[1−4] Attempts have been reported[5−11] aiming at controlling properties of liquid crystals by photochemical reactions of the dopants. It has been demonstrated that the stability of phases can be modulated by photochemical reactions following excitations of photoactive dye molecules. In particular, the photochemically driven trans−cis isomerization reaction occurring in azobenzene derivatives dissolved in liquid-crystalline matrixes has been reported to modify the temperature of the nematic−isotropic (N−I) phase transition.[12−15] Ruslim and Ichimura[12] employed the Flory−Huggins theory to explain the phase behavior of a liquid-crystal-azobenzene derivative system due to the photoisomerization of the dopant.

Although reports on light-driven phase transitions in dye-doped liquid crystals can be found in the literature,[12−19] little is known about relations between the photochromic process and the phase transition. Sung at al.,[19] having examined the phase behavior of pentylcyanobiphenyl (5CB) doped with 4-butyl-4′-methoxyazobenzne (BMAB), found a dependence of the dynamics of the photochemically induced phase transition on parameters of domains of the isotropic phase formed upon the photoinduced trans−cis isomerization of the dye.

The aim of this contribution is to present results of kinetic studies of the isomerization of photochromic 4-fluoro-4′-methoxyazobenzene (FMA) dissolved in 5CB and of the isomerization-induced phase change in the system. The system under study was selected because of a compatibility of molecular dimensions of the host and guest molecules, as may be deduced from a comparison of the formulas of the molecules under study, shown in Figure 1.

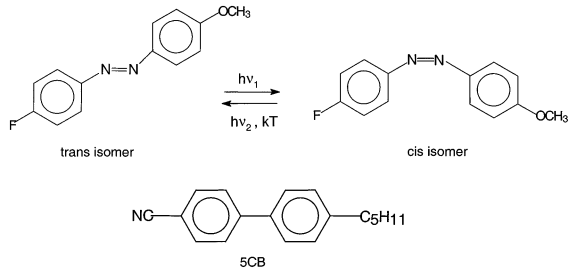

Figure 1. Chemical formulas of the molecules under study.

Experimental Section

FMA has been obtained from Dr Z. Galewski (University of Wrocław). Synthesis and purification of the material has been described elsewhere.[20] Solutions of FMA in 5CB (Merck) were prepared in two concentration ranges: the mole fraction of FMA (x_{azo}) in those used in spectroscopic and kinetic measurements was of the order of 10^{-3}, whereas x_{azo} in samples used in optical experiments ranged between 0 and 0.022. The samples were placed in cells 5 or 10 μm thick.

The measurements of UV−vis absorption spectra and of the isomerization kinetics were performed with a Perkin-Elmer Lambda 20 spectrophotometer. Irradiation of the samples was done in situ, with a high-pressure mercury lamp (total nominal power 200 W) and appropriate combinations of color glass filters. The radiation was supplied to the sample using quartz light guide. The isomerization was measured by monitoring changes of the spectra.

To investigate optical properties of the system, a polarizing microscope Olympus BX60 was used, equipped with a Linkam 350 thermostated stage. UV and vis irradiation were performed

* To whom correspondence should be addressed. E-mail: matczyszyn@kchf.ch.pwr.wroc.pl. Fax: (+48-71)320-33-64.

10.1021/jp026966+ CCC: $25.00
Published on Web 05/29/2003

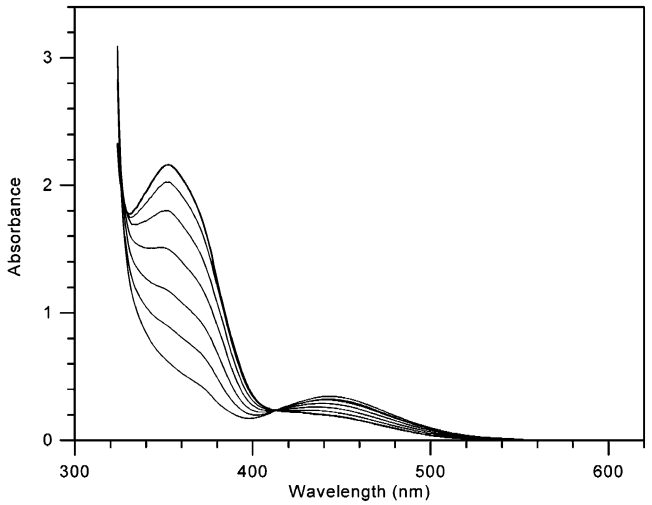

Figure 2. Absorption spectra of FMA in 5CB. The uppermost spectrum (dashed curve) is that of a pristine sample; the following spectra have been measured after 25, 105, 270, 400, 660, and 1800 s of irradiation with the 365 nm light. The absorption edge at ca. 330 nm is due to the absorption of 5CB.

in situ with a mercury lamp or a halogen lamp via appropriate combinations of color filters.

The calorimetric measurements were carried out with a Perkin-Elmer DSC7 scanning calorimeter, covering the temperature range of the N−I transition of 5CB (ca. 290 to 315 K). Typically, masses of the samples used in the DSC experiments ranged between ca. 0.1 and 5 mg.

Results

The spectra of FMA in *n*-heptane and DMSO and in 5CB are shown in Figure 2. The spectra of the stable form exhibit features characteristic of parent azobenzene: a strong $\pi-\pi^*$ band at ca. 350 nm and a much weaker broad band peaking at ca. 440 nm, due to the $n-\pi^*$ transition. Under irradiation with UV light ($\lambda = 365$ nm), the stable trans form of the azobenzene derivative converts into the metastable cis form (cf. Figure 1), the isomerization manifesting itself in a decrease of the intensity of the 350 nm band, and a build-up of the $n-\pi^*$ band, accompanied by its blue shift. The reverse reaction may occur either thermally or upon illumination with visible light ($\lambda =$ 440 nm). The isomerization kinetics was investigated by monitoring the absorbance of *trans*-FMA at ca. 350 nm (see infra). The evolution of the absorbance due to the photochemical trans−cis isomerization of FMA in 5CB, measured at a few temperatures, is shown in Figure 3a−c. No detailed studies of the kinetics of these reactions were performed, the experiments reported in this section aiming only at elucidating basic features of microscope experiments described in the following parts of this paper.

The kinetics of the thermally driven cis−trans isomerization was studied in more detail, both in common solvents of various polarities (*n*-heptane and DMSO) and in 5CB. The liquid crystal is known to undergo a phase transition between the nematic and isotropic phases (N−I transition) at 308 K.[21,22] The isomerization kinetics was measured in the temperature regions of the stability of both the nematic and isotropic phases of 5CB. Representative curves, showing the evolution of the absorbance due to the thermally driven cis−trans isomerization of FMA in 5CB, measured at a few temperatures, are shown in Figure 4a.

We also carried out microscopic observations of the phase transition in the solutions of FMA in 5CB. Experiments reported

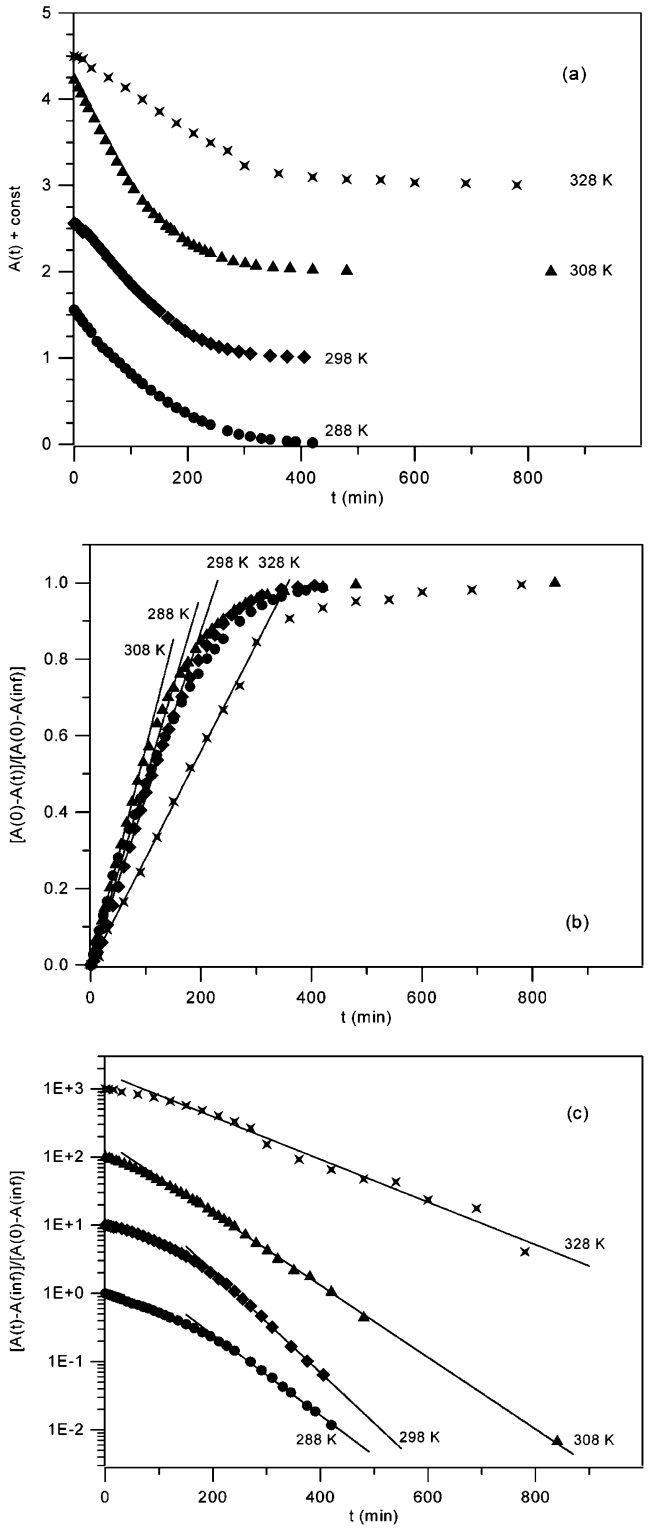

Figure 3. (a) Temporal changes of the absorbance of FMA in 5CB, due to the photochemical trans−cis isomerization, monitored at 350 nm. The parameter is temperature. The curves have been vertically displaced. (b) Data from Figure 3a, re-plotted in the coordinates resulting from eq 8. (c) Data from Figure 3a, re-plotted in the coordinates resulting from eq 4. The curves have been vertically displaced.

in this paper were performed on a diluted system containing 1 wt % of the solute ($x_{azo} = 0.011$), to avoid any possible effects associated with aggregation of the dye. It was found that the isomerization reaction may trigger an apparent nematic-to-isotropic phase transition of solutions at temperatures substan-

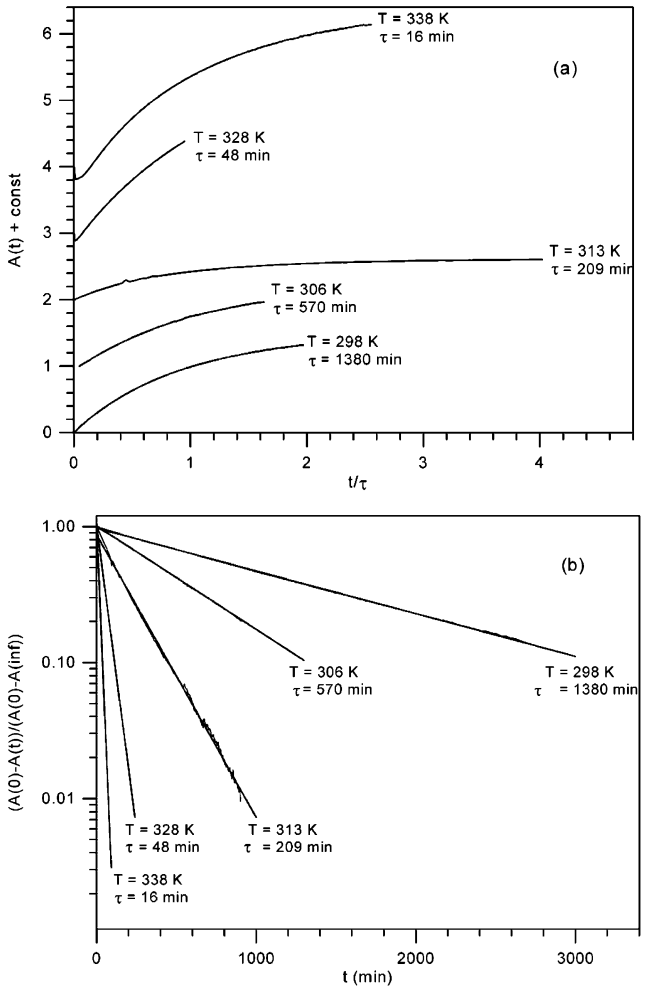

Figure 4. (a) Temporal changes of the absorbance of FMA in 5CB, due to the thermally driven cis−trans isomerization, monitored at 350 nm, measured at various temperatures. Only a few curves are shown. The curves have been vertically displaced and normalized. The parameters are temperature T and the time constant $\tau = 1/k_{ZE}^{dark}$. (b) Data from Figure 4a, re-plotted in the coordinates resulting from eqs 7 and 8. The time constants $\tau = 1/k_{ZE}^{dark}$ are calculated at each temperature from the slopes of the decays.

tially lower than the thermodynamic transition temperature of pure 5CB, even at concentrations as low as those used in our experiments. Upon illumination with the 365 nm radiation, one could notice the isotropic phase appear well below the temperature of the thermodynamic phase transition of pure 5CB (cf. Figure 5); the effect was observed even at 290 K. The incubation time of the isotropic phase (the time necessary to detect first droplets of the isotropic phase, hereafter denoted t_1) was found to depend on the temperature, light intensity, and concentration of the dye. The temperature dependence of the incubation time is shown in Figure 6a. A further illumination was found to result in the disappearance of the nematic phase inside the illuminated region of the sample; a precise determination of the characteristic time proved, however, difficult. In the darkness, the samples undergo a reverse process: after a certain time (t_2), the nematic phase was found to reappear, and after the time t_3, the last portions of the isotropic phase disappeared. Both, the time of reappearance of first droplets of the nematic phase (t_2) and time of disappearance of last portions of the isotropic phase (t_3) were temperature-dependent, as is shown in Figure 6b.

Discussion

Isomerization Kinetics. The isomerization of azobenzene and its derivatives, presented in Figure 1, is, from the kinetic point of view, a process approaching equilibrium

$$E \underset{k_{ZE}}{\overset{k_{EZ}}{\rightleftharpoons}} Z$$

In the above scheme, *E* and *Z* represent the trans and cis forms of the isomerising molecule, and *k*'s are effective rate constants. A general equation describing the temporal evolution of the concentrations of both forms can, in principle, be found. It would be, however, more convenient to derive solutions describing particular processes discussed in this paper.

(i) trans−cis Isomerization under Illumination with Visible Light or in the Dark. Under the illumination with the 440 nm light or in the darkness, $k_{EZ} < k_{ZE}$; in general, however, the inequality is not strong enough to neglect any of the rate constants a priori. Moreover, because the absorption of the visible light is rather weak (cf. Figures 2 and 3), one may assume a uniform illumination of the sample bulk. Under these assumptions, the kinetic equation reads

$$\frac{dx_Z}{dt} = -k_{ZE}x_Z + k_{EZ}x_E \tag{1}$$

where k_{ZE} and k_{EZ} are effective rate constants

$$k_{ZE} = k_{ZE}^{dark} + \kappa_{ZE}^{440}I^{440} \tag{2a}$$

$$k_{EZ} = k_{EZ}^{dark} + \kappa_{EZ}^{440}I^{440} \tag{2b}$$

Here, κ are parameters including material and system constants (cf. eq 8), I is the intensity of the exciting light inciding onto the sample, and k_{dark} stands for the rate constants of the thermally driven cis−trans and trans−cis reactions, respectively (the latter one being negligibly small). The temperature dependences of the thermally driven reactions are expected to follow the Arrhenius equation

$$k_i^{dark} = \nu_i \exp\left(-\frac{E_i}{RT}\right) \tag{3}$$

where i = EZ or ZE, E_i is the activation energy of the reaction, and ν_i is its preexponential (frequency) factor. Under illumination, however, the second terms in eqs 2a and 2b prevail, and the effective rate constants are expected to be weakly dependent on temperature.

Keeping in mind that $x_E(0) + x_Z(0) = x_E(t) + x_Z(t) = x_E(\infty) + x_Z(\infty) = x_{azo}$, one obtains

$$\frac{x_Z(t) - x_Z(\infty)}{x_Z(0) - x_Z(\infty)} = \exp(-(k_{EZ} + k_{ZE})t) \tag{4}$$

In the above equations, $x_Z(0)$, $x_Z(t)$, and $x_Z(\infty)$ denote, respectively, the initial and momentary mole fractions of the cis isomer and the mole fraction in the equilibrium (i.e., in the thermodynamic equilibrium or after attaining a photostationary state).

As was mentioned in the preceding section, the temporal changes of the concentration of both forms of FMA were monitored by measuring the absorbance at ca. 350 nm, i.e., at the maximum of the $\pi-\pi^*$ absorption of the trans form. Making

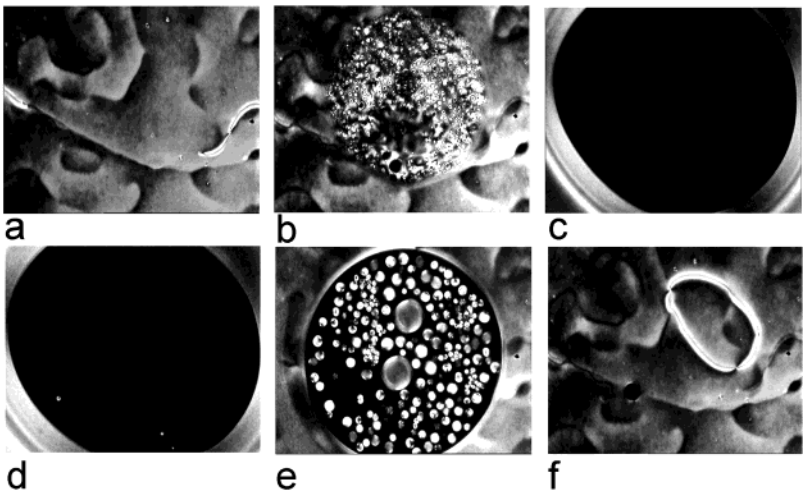

Figure 5. Solution of FMA in 5CB observed under a polarizing microscope. $x_{azo} = 0.011$, $T_{exp} = 306$ K. (a) Pristine sample prior to illumination (nematic phase); (b and c) illumination with 365 nm radiation: (b) appearance of first droplets of the isotropic phase (characteristic time t_1); (c) complete disappearance of the nematic phase; (d−f) the sample kept in the dark: (d) reappearance of first droplets of the nematic phase (characteristic time t_2); (e) nematic phase embedded in the isotropic phase; (f) disappearance of the isotropic phase (characteristic time t_3).

use of the Lambert−Beer law, one may show that the following relations, valid for both directions of the reaction, are fulfilled:

$$\frac{x_E(t) - x_E(\infty)}{x_E(0) - x_E(\infty)} = \frac{x_Z(t) - x_Z(\infty)}{x_Z(0) - x_Z(\infty)} = \frac{A(t) - A(\infty)}{A(0) - A(\infty)} \qquad (5)$$

where $A(0)$, $A(t)$, and $A(\infty)$ denote the initial and momentary absorbances and the absorbance in the equilibrium. The data from Figure 4a, redrawn in the new coordinates, resulting from the combination of eqs 4 and 5 are shown in Figure 4b. The results obtained for both the thermal and photochemical cis−trans isomerization were found to reasonably follow the semilogarithimic dependences. The kinetics of the latter reaction, however, was not studied in detail, the attention being focused on the kinetics of the thermally driven cis−trans reaction and the temperature dependence of the respective rate constant. In this case, $k_{EZ}^{dark} \ll k_{ZE}^{dark}$, and eq 4 simplifies to

$$x_Z(t) \approx x_Z(0) \exp(-k_{ZE}^{dark} t) \qquad (4a)$$

As expected, the thermal cis−trans reaction follows the first-order kinetics (cf. Figure 4b). Figure 7 shows the temperature dependencies of the rate constant k_{dark} in various solvents. As comes from the figure, the Arrhenius dependence is fulfilled for FMA dissolved in common solvents and for FMA in 5CB outside the phase transition region. It is interesting to note that, outside the phase transition region, the rate constants measured in the solution in 5CB fulfill a common Arrhenius dependence irrespective of whether measured in the range of stability of the nematic or isotropic phase. This feature seems to demonstrate that the long-range order of the matrix does not significantly influence the isomerization of the solute. It should be also pointed out that the sequence of the parameters of the Arrhenius equation describing the temperature dependencies of the cis−trans thermal isomerization seems to scale with the positions of maxima of the $\pi-\pi^*$ absorption of the trans form (cf. Table 1). The apparent correlation should be checked more thoroughly but, if confirmed, it would point out to the sensitivity of the isomerization barrier to the polarity of the solvent.

In the vicinity of the phase transition temperature, we observed an erratic non-Arrhenius behavior of the measured rate constants, significantly exceeding the experimental error. Because a similar experiment performed on E7 (a liquid-crystalline mixture of cyanobiphenyls exhibiting no phase transition in the temperature range of interest) revealed no such an effect, we

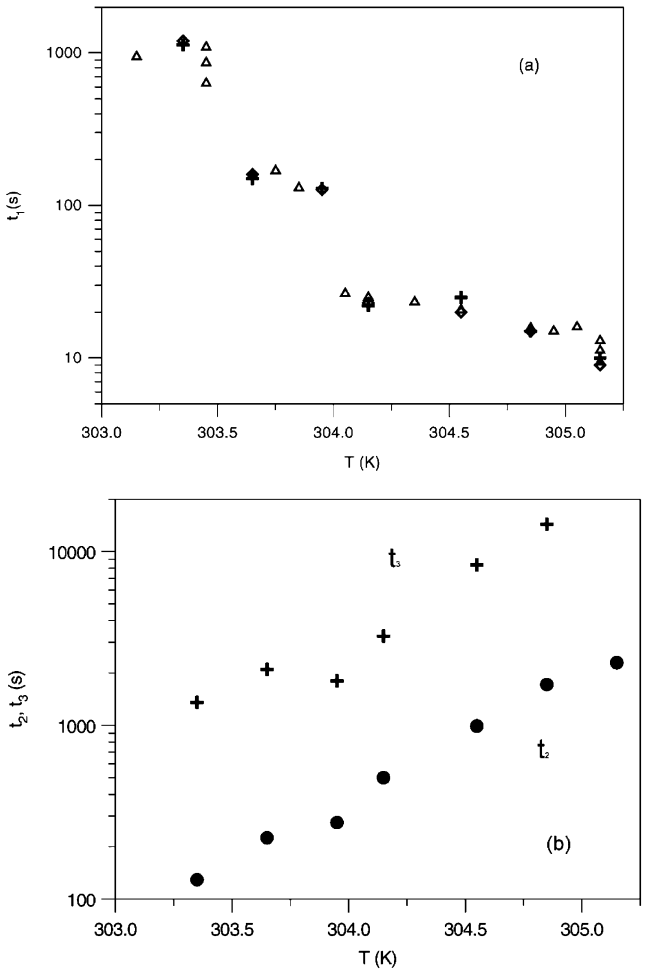

Figure 6. Temperature dependencies of the characteristic times of the phase transition in solutions containing FMA dissolved in 5CB. (a) Incubation time (t_1) of the N−I phase transition triggered by the photoinduced trans−cis isomerization. Runs performed on different samples are represented by different symbols. (b) I−N phase transition triggered by the thermal cis−trans isomerization of FMA. Full circles: time of reappearance of the nematic phase (t_2); crosses: time of disappearance of the isotropic phase (t_3).

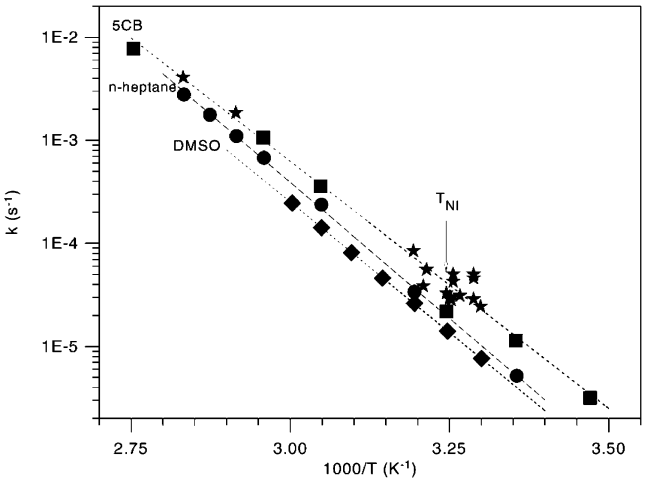

Figure 7. Temperature dependence of the rate constant of the thermal cis−trans isomerization of FMA in "conventional" solvents and in 5CB. Note the deviations from the Arrhenius dependence in the vicinity of the phase transition temperature of 5CB (indicated by the vertical dotted line). Runs performed on different samples are represented by different symbols. The parameters determined from the Arrhenius fits to the experimental data are given in Table 1.

TABLE 1: Parameters Determined from the Arrhenius Fits to the Temperature Dependences of the Thermal Isomerization Rates of FMA in Various Solvents[a]

solvent	E_a (kJ/mol)	ν (10^{11} s^{-1})	λ (nm)
n-heptane (nonpolar)	101	25.5	343
DMSO (polar)	97	3.7	351
5CB (liquid crystal)	92	1.5	353

[a] For comparison, positions of the maxima of the $\pi-\pi^*$ absorption of the trans form have also been given.

tentatively associate it with the phase transition in the liquid crystalline matrix. At present, however, we cannot put forward any model quantitatively explaining the observed anomaly.

(ii) Photochemical trans−cis Isomerization, Illumination with UV Radiation. In this case, $k_{EZ} \gg k_{ZE}$, and at initial stages of the process, the absorbance is high enough (cf. Figure 3a) to fulfill the condition of a complete absorption of the incident light. Hence

$$\frac{dn_E}{dt} = -\eta_{EZ} I^{365} \tag{6}$$

where n_E is the number of trans molecules in the reacting system, η_{EZ} is the quantum efficiency of the trans−cis photochemical conversion, and I^{365} is the intensity of the exciting light inciding onto the sample. At any moment, n_E is related to the mole fraction of trans molecules by the simple relation

$$n_E = \frac{V\rho N_A}{M_{5CB}} x_E \tag{7}$$

where V is the active volume of the sample used in our kinetic experiments (7×10^{-4} cm^3), ρ and M_{5CB} are the density and molar mass of 5CB, and N_A is the Avogadro number. After simple manipulations, and making use of the Lambert−Beer law, one arrives at the equation

$$\frac{A(0) - A(t)}{A(0) - A(\infty)} = \frac{M_{5CB}\eta_{EZ} I^{365}}{V\rho N_A x_{azo}} t = \frac{k_{EZ}}{x_{azo}} t \tag{8}$$

describing the 0th order kinetics, with the effective rate constant k_{EZ} linearly depending on the light intensity. The equation holds as long as the initial assumption concerning the complete absorption of the incident light is fulfilled.

The data of Figure 3a, re-drawn in the coordinates resulting from eq 8, are shown in Figure 3b. The effective rate constant extracted from the spectroscopic experiments proves almost temperature-independent amounting to ca. $(7\pm2) \times 10^{-5}$ s^{-1} within the range of temperatures covered by our experiments and for the employed concentration of the dye and illumination intensity. The value obtained can serve as a consistency test as it allows for an estimation of light intensity absorbed by the sample. Taking $\eta_{EZ} = 0.12$, i.e., equal to that of parent azobenzene[23] and $\rho = 1$ g/cm^3,[24] one arrives at $I \approx (1\pm0.3) \times 10^{16}$ quanta/s, i.e., at ca. (5 ± 1) mW at 365 nm. This value, albeit quite low, does not seem unphysical in view of severe losses due to scattering, use of filters, and an unoptimized geometry of the system.

If the absorption of the exciting light decreases to a sufficiently low value, the reaction starts following the first-order kinetics as is shown in Figure 3c. The effective rate constants, determined from the fits to the long-time sections of the experimental dependencies, are practically temperature-independent and amount to $(6 \pm 2) \times 10^{-4}$ s^{-1} within the range of temperatures covered by our experiments and for the employed illumination intensity.

Phase Transition in the Dye-Doped Liquid Crystal. The calorimetric measurements point to a good miscibility (and hence, a good compatibility) of 5CB and *trans*-FMA. Up to the upper limit of the concentrations of the dye ($x_{azo} \leq 0.022$), the temperature of the onset of the N−I phase transition was found to fulfill the relation

$$T = T_{NI} - \xi x_E^N \tag{9}$$

with $T_{NI} = 308.1$ K, and $\xi = 21.1$ K. At the temperature T, first portions of the isotropic phase appear on heating the samples; the concentration of the dye in the other phase can be estimated from thermodynamic relations. Discussing a similar problem, Ruslim and Ichimura[12] followed the approach put forward by Kronberg et al.,[25,26] based on the Flory−Huggins theory. In our case, the compatibility of shapes of the host and guest molecules, as well as low concentrations of the guest used in our experiments, allow us to employ the Van Laar-Hildebrand-type equation valid for ideal solutions[27]

$$\ln\left(\frac{x_{5CB}^N}{x_{5CB}^I}\right) = -\frac{\Delta H_{NI}^0}{R}\left(\frac{1}{T_{NI}} - \frac{1}{T}\right) \tag{10}$$

Combining eqs 9 and 10, and remembering that $x_{5CB} = 1 - x_E \approx 1$, one arrives at the equation

$$x_E^I = x_E^N\left(1 + \frac{\Delta H_{NI}^0}{RT_{NI}^2}\xi\right) = \gamma x_E^N \tag{11}$$

the effective coefficient of distribution γ being defined by the expression in the brackets of eq 11 and ξ being the parameter used in eq 9. Taking $\Delta H_{NI}^0 = 738$ J/mol (average from our measurements, well comparing with the largest value reported in the literature[12]), one obtains $\gamma = 1.01$. Thus, there is practically no difference in the dye concentrations in the coexisting phases.

The dependence of the temperature of the nematic-to-isotropic phase transition on the isomerization reaction can be rationalized based on a simple model taking into account differences in the

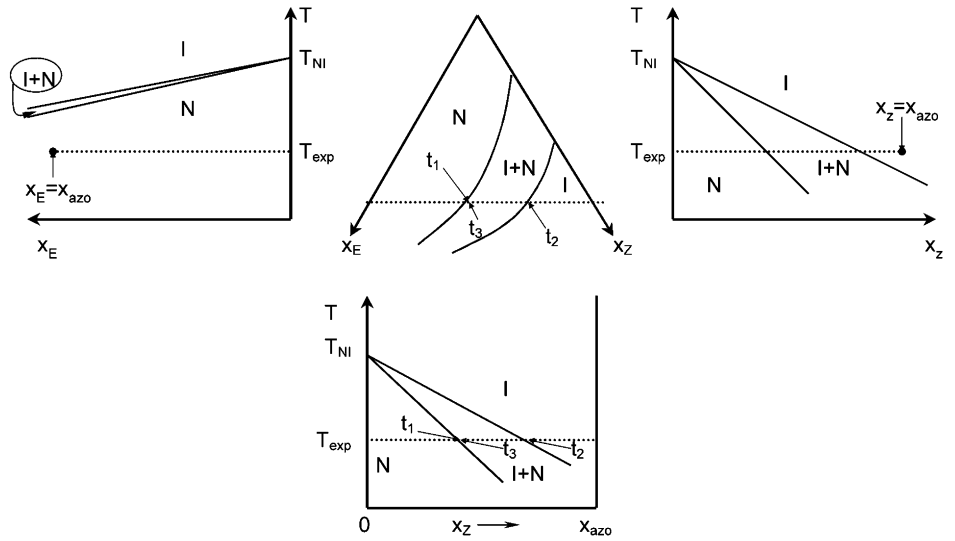

Figure 8. Tentative representation of the phase diagram of the system under study. The central part represents a fragment of the Gibbs triangle of the ternary system 5CB/*trans*-FMA/*cis*-FMA taken at a constant temperature $T_{exp} < T_{NI}$ (indicated by the dashed lines on the $T-x$ phase diagrams). The side diagrams are $T-x$ ones of binary systems 5CB/*trans*-FMA (on the left) and 5CB/*cis*-FMA (on the right). The bottom diagram is a pseudo-binary one, taken at $x_E(t) + x_Z(t) = x_E(0) + x_Z(0) = x_{azo} =$ constant (indicated by the dashed line on the ternary diagram). The symbols I and N denote the stability regions of the isotropic and nematic phases, respectively, t_i are the characteristic times discussed in the text.

solubility of FMA in 5CB, because of the differences in molecular shapes of the trans and cis forms of the dye. The photochemical trans−cis reaction results in production of cis molecules, incompatible with 5CB, and hence poorly soluble in the matrix. Thus, the increase of the concentration of the former molecules should result in saturation of the solution, followed by a phase separation and, finally, by a disappearance of the nematic phase. Schematically, the process can be illustrated with the phase diagram shown in Figure 8.

The validity of the model can be assessed as the concentration of cis molecules can be calculated from the equations given above provided the initial concentrations and the rate constants are known. Because in the thermal equilibrium practically the whole amount of the dye exists in the form of the trans isomer, one may derive an equation, analogous to eq 8, relating t_1 to the critical concentration of the cis isomer in the sample (i.e., the concentration of the cis isomer in the saturated solution)

$$x_Z(t_1) \approx k_{EZ} t_1 \tag{12}$$

Thus, the incubation time t_{1ph} is directly related to the concentration of *cis*-FMA in its saturated solution in the nematic phase of 5CB. In principle, the equation could be used to estimate x_Z; unfortunately, the equation cannot be employed directly, as the intensity of the light absorbed by the sample in our microscope experiments could not be reliably determined. Moreover, the validity of the above equation is limited to a short initial period of irradiation, when the absorbance at 365 nm is high enough as was shown in the preceding section.

Changes of the concentration of *cis*-FMA during the cis−trans reaction are described by eqs 4 and 5. Consequently, the time of reappearance of first droplets of the nematic phase (t_2) should be related to the concentration of *cis*-FMA in its saturated solution in the isotropic phase of 5CB, whereas the time of disappearance of last portions of the isotropic phase (t_3) should be related to the concentration of *cis*-FMA in its saturated solution in the nematic phase of 5CB. Under illumination with the visible light, the photochemical component of k_{ZE} prevails; hence, the dependences of the characteristic times on temperature should follow only the temperature dependence of the solubility of *cis*-FMA.

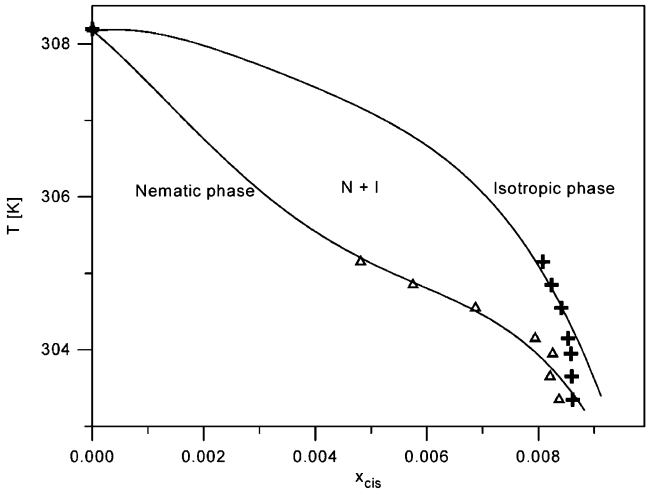

Figure 9. Pseudo-binary phase diagram 5CB/FMA (a cross-section of the ternary system taken at $x_{azo} = 0.011$) deduced from the microscope experiments.

If the reverse reaction occurs in the dark, then the critical concentrations can be determined employing eq 4a: the characteristic times of the appearance and disappearance of the phases, determined in our experiments, can be used to construct a pseudo-binary phase diagram of the system taken for $x_Z + x_E = x_{azo} =$ constant (the horizontal axis corresponds to the horizontal dashed line in the Gibbs triangle shown in Figure 8)

$$x_Z(t_2) = x_Z(0) \exp(-k_{ZE}^{dark} t_2) \tag{13}$$

$$x_Z(t_3) = x_Z(0) \exp(-k_{ZE}^{dark} t_3)$$

with k_{ZE}^{dark} at a given temperature available from the experiments described in the preceding section.

The resulting diagram, calculated assuming $x_Z(0) = 0.8x_{azo}$, is shown in Figure 9. It should be stressed that the lines shown in the figure should be taken only as a semiquantitative indication of the possible course of the phase equilibrium lines as the experimental setup used in our experiments did not allow for a reliable determination of characteristic times shorter than ca. 10 s.

Final Remarks

The results obtained explain, on a semiquantitative basis, the photochemically driven phase transition appearing below the thermodynamic temperature. One should realize, however, that the model contains several simplifications. First, the model neglects all but chemical processes occurring in the system, neglecting all effects associated with the diffusion of the dye between the illuminated and dark parts of the sample. Second, in the calculations employing eq 13 we used average values of the temperature dependent k_{ZE}^{dark}, totally neglecting the deviations from the Arrhenius behavior observed just around the phase transition. We believe, however, that all these factors may qualitatively modify the dependence but its general form will remain unchanged.

Our results are in a qualitative agreement with those of Sung et al.[19] Some differences in the behavior of the samples (and in particular in the textures) are, most probably, due to different surface interactions: in our experiments, the liquid crystal matrixes were contacted directly with glass surfaces, whereas Sung et al.[19] used polyimide alignment layers.

The experiments described in this paper demonstrate that the occurrence of "photoinduced phase transitions" reported for photochromic dye-doped liquid crystals can be rationalized taking into account different compatibilities (and hence different solubilities) of both forms of photochromic systems. The effects observed by us in the *cis*-FMA/*trans*-FMA/5CB should be common to many photochromic systems dissolved in liquid crystals, in the vicinity of a phase transition of the matrix.

Acknowledgment. The authors thank Dr. Z. Galewski (University of Wrocław) for the gift of FMA used in the present study. Merck KGaA are greatly acknowledged for the gift of 5CB. The research reported in this paper was supported by the Polish State Committee for Scientific Research (Grant No. 7 T09A 012 21).

References and Notes

(1) Irie, M., Ed.; *Photo-Reactive Materials for Ultrahigh-Density Optical Memory*; Elsevier: Amsterdam, 1994.

(2) Yeh, C. *Applied Photonics*; Academic Press: San Diego, CA, 1994.

(3) Blinov, L. M.; Chigrinov, V. G. *Electrooptic Effects in Liquid Crystal Materials*; Springer-Verlag: New York, 1996.

(4) Nathanson, A., Ed.; *Azobenzene-Containing Materials*; *Macromol. Symp.* **1999**, *137*, 1−165.

(5) Ikeda, T.; Tsutsumi, O. *Science* **1995**, *268*, 1873.

(6) Ikeda, T.; Sasaki, T.; Ichimura, K. *Nature* **1993**, *361*, 428.

(7) Wu, Y.; Mamiya, J.; Kanazawa, A.; Shiono, T.; Ikeda, T.; Zhang, Q. *Macromolecules* **1999**, *32*, 8829.

(8) Yamamoto, T.; Ohashi, A.; Yoeyama, S.; Hasegawa, M.; Tsutsumi, O.; Kanazawa, A.; Shiono, T.; Ikeda, T. *J. Phys. Chem. B* **2001**, *105*, 2308.

(9) Ogura, K.; H. Hirabayashi, H.; Uejima, A.; Nakamura, K. *Jpn. J. Appl. Phys.* **1982**, *21*, 969.

(10) Janossy, I.; Szabados, L. *Phys. Rev. E* **1998**, *58*, 4598.

(11) Lee, H.-K.; Kanazawa, A.; Shiono, T.; Ikeda, T. *Chem. Mater.* **1998**, *10*, 1402.

(12) Ruslim, Ch.; Ichimura, K. *J. Mater. Chem.* **1999**, *9*, 673.

(13) Tsutsumi O., Kanazawa A.; Shiono, T.; Ikeda, T.; Park, L.-S. *Phys. Chem. Chem. Phys.* **1999**, *1*, 4219.

(14) Prasad, K.; Nair, G. G. *Adv. Mater.* **2001**, *13*, 40.

(15) Ikeda, T.; Sasaki, T.; Kim, H.-B. *J. Phys. Chem.* **1991**, *95*, 509.

(16) Kurihara, S.; Ikeda, T.; Sasaki, T.; Kim, H.-B.; Tazuke, S. *J. Chem. Soc., Chem. Commun.* **1990**, 1751.

(17) (a) Ikeda, T.; Kurihara, S.; Karanjit, D. B.; Tazuke, S. *Macromolecules* **1990**, *23*, 3938. (b) Ikeda, T.; Horiuchi, S.; Karanjit, D. B.; Kurihara, S.; Tazuke, S. *Macromolecules* **1990**, *23*, 36. (c) Ikeda, T.; Horiuchi, S.; Karanjit, D. B.; Kurihara, S.; Tazuke, S. *Macromolecules* **1990**, *23*, 42.

(18) Sandhya, K. L.; Prasad, S. K.; Nair, G. G. *Phys. Rev. E* **2001**, *64*, 041702.

(19) Sung, J.-H.; Hirano, S.; Tsutsumi, O.; Kanazawa, A.; Shiono, T.; Ikeda, T. *Chem. Mater.* **2002**, *14*, 385.

(20) (a) Galewski, Z. *Liquid Crystalline Polymorphism of Schiff Bases and Azobenzenes*; University of Wrocław: Wrocław, Poland, 1999, (b) Galewski, Z. *Polish J. Chem.* **1999**, *9*, 1503.

(21) Gray, G. W.; Harrison, R. J.; Nash, J. A.; Constant, J.; Hulme, D. S.; Kirton, J.; Raynes, E. P. *Liq. Cryst. Ordered Fluids* **1974**, *2*, 617.

(22) Kneppe, H.; Schneider, F.; Sharma, N. H. *Phys. Chem.* **1981**, *85*, 784.

(23) Zimmerman, G.; Chow, L.-Y.; Paik, U.-J. *J. Am. Chem. Soc.* **1958**, *80*, 3528.

(24) Sen, S.; Brahma, P.; Roy, S. K.; Mukherjee, D. K.; Roy, S. B. *Mol. Cryst. Liq. Cryst.* **1987**, *100*, 327.

(25) Kronberg, B.; Patterson, D. J. *Chem. Soc., Faraday Trans. II* **1976**, *72*, 1687.

(26) Kronberg, B.; Gilson, D. F. R.; Patterson, D. *J. Chem. Soc., Faraday Trans II* **1976**, *72*, 1673.

(27) Swalin, R. A. *Thermodynamics of Solids*; J. Wiley: New York, 1962; Chapter 11.4.